Evidence for Successive Doping-Induced Dimensionality Transitions in the Spin-Chain Compound $Ca_{2+x}Y_{2-x}Cu_5O_{10}$

Michelle D. Chabot and John T. Markert
Department of Physics, University of Texas, Austin, Texas 78712
(Received 19 June 2000)

We report the results of heat capacity, SQUID magnetometry, and x-ray diffraction studies of polycrystalline and magnetically aligned $Ca_{2+x}Y_{2-x}Cu_5O_{10}$, a quasi-1D compound. As holes are doped into the chains from $x = 0-2$, the data indicate a change from 3D long-range order to 1D chain behavior to cluster behavior. We quantitatively model the magnetic and thermal properties of heavily doped $Ca_4Cu_5O_{10}$ in terms of spin clusters. Anisotropic susceptibility data indicate a doping-independent easy axis of magnetization perpendicular to the planes containing the chains; also, a spin-flop transition is observed, providing a measure of the anisotropy field.

DOI: 10.1103/PhysRevLett.86.163 PACS numbers: 75.40.Cx, 75.10.Jm, 74.72.Jt

Since the discovery of high T_c superconductivity in cuprate materials, low-dimensional copper-oxide systems have received a great deal of attention. In particular, there is interest in the magnetic properties of spin-chain compounds due to the enhancement of quantum fluctuations in one dimension. In these quasi-1D systems, long-ranged (3D) order can occur only through finite coupling between the chains. Such 3D antiferromagnetic order has been found in the spin-chain compounds Ca_2CuO_3 [1] and Sr_2CuO_3 [1,2], which have strong antiferromagnetic interactions due to the 180° Cu-O-Cu coupling in the linear chains of corner-sharing CuO_2 squares. Of more interest here are the compounds which contain chains of edge-sharing CuO_4 squares with nearly 90° Cu-O-Cu bonds. The spin-chain compound $CuGeO_3$, which undergoes a spin-Peierls transition [3], exhibits long-ranged antiferromagnetic order when lightly doped [4,5]. Another system that has attracted considerable attention is based on $Sr_{14}Cu_{24}O_{41}$, a quasi-1D compound containing planes of both two-leg ladders and simple chains. Evidence for a dimerized state has been observed in this system, resulting in the appearance of a spin gap [6]. The formation of this spin gap has been found to be greatly affected by hole doping [7,8].

Recently, new cuprates have been synthesized which consist only of linear chains that are highly doped with holes. $Sr_{0.73}CuO_2$ (formal copper valence of +2.54) has been reported to exhibit long-ranged weak ferromagnetic order, with indications of possible dimerization [9,10]. Dimerlike behavior has also been found in $Ca_{0.85}CuO_2$ (copper valence of +2.30), with evidence of a spin gap attributed to the incommensurate structure [11]. Like $Sr_{0.73}CuO_2$, $Ca_{0.85}CuO_2$ is reported to undergo a transition to long-range antiferromagnetic order [10,12]. Recently, the similar spin-chain compound $Ca_{2+x}Y_{2-x}Cu_5O_{10}$ has been synthesized with a variable doping level ranging from $x = 0$ to $x = 2$ (formal copper valences from +2 to +2.4) [13]. This wide range of hole doping makes this compound particularly interesting for detailed study. The undoped compound exhibits long-range antiferromagnetic order [14–17], but the nature of the magnetic behavior for the substantially hole-doped compounds has not yet been determined.

In this Letter, we report the magnetic susceptibility and heat capacity of polycrystalline and grain-aligned $Ca_{2+x}Y_{2-x}Cu_5O_{10}$. This structure consists of quasi-1D CuO_2 chains separated by insulating planes containing Ca and Y [13]. As holes are introduced into the chains, we confirm that the peak in the magnetic susceptibility decreases and broadens, reflecting a change in the magnetic ordering. We find that the specific heat anomaly of the undoped compound broadens at the midrange doping level and exhibits a double-peaked behavior for the maximally doped compound. We model these phenomena in terms of quasi-1D Heisenberg behavior for the mid-doping range and microscopic segregation of the chains into finite spin clusters for the maximally doped compound, suggesting there are doping-induced dimensionality transitions in $Ca_{2+x}Y_{2-x}Cu_5O_{10}$.

Samples were prepared by conventional solid state reaction, starting with high-purity predried Y_2O_3, $CaCO_3$, and CuO. All samples were ground and fired in air at 900 °C multiple times. The undoped $x = 0$ compound was then reground, pressed, and fired in air at 1000 °C for over 48 h. This step was repeated once. The doped samples were reground, pressed, and fired in high-pressure oxygen (1.7×10^7 Pa) at 1000 °C for over 48 h. The procedure was then repeated. Room temperature x-ray diffraction data are in good agreement with previous results [13]; no impurity phases were detected at the <1% level, and the lattice constants varied linearly with the doping level. Magnetic measurements were made with a Quantum Design MPMS SQUID magnetometer. Specific heat data were measured using an RMC calorimeter and the thermal relaxation method [18]. For anisotropy studies, samples were aligned by mixing finely ground powder with Stycast 1266 epoxy and placing the mixture in an 8.2 T magnetic field for over 24 h.

Figure 1 shows the results of the magnetic susceptibility measurements made on polycrystalline samples. The results were found to be independent of applied field. As found previously, the undoped compound exhibits long-ranged antiferromagnetic order, with $T_N = 29$ K [13]. (The small shoulder barely observable at $T = 12$ K is due to the presence of trace amounts of $Y_2Cu_2O_5$.) As doping increases to $x = 1$, the location of the peak decreases to $T_N \approx 20$ K. With further doping, the peak broadens and the location of the maximum increases. For the maximally doped compound, the curve exhibits a broad maximum at $T \approx 30$ K. Upon closer examination, we observe a shoulder in the data for the yttrium-free $x = 2$ compound at $T \approx 11$ K, as shown in the inset of Fig. 1. A similar feature has also been found to exist in the spin-chain compound $Ca_{0.83}CuO_{2-\delta}$ [12]. This broad peak and shoulder are indications of the changing nature of the magnetic order, and we propose that they are due to a microscopic segregation of the chain spins, as will be discussed shortly.

To further investigate the magnetic properties of the chains, specific heat measurements were made for the various doping levels and are shown in Fig. 2(a). As expected for long-ranged antiferromagnetic order, a large, sharp specific heat anomaly is observed for the undoped sample at the Neél temperature. The three-dimensional nature of the $x = 0$ peak is clear in the lattice-subtracted specific heat of Fig. 2(b), where $C_{\text{lattice}} \approx \beta T^3$ with $\beta = 1.0$ mJ/mole K^4 has been used. However, as holes begin to be introduced into the chains ($x = 1$), the specific heat peak becomes small and very wide. It would be implausible to attribute this behavior to a wide and continuous distribution of different regions of antiferromagnetic order with different T_N's; even for a dilute or partially frustrated system, the transition to long-range order would occur at a single temperature. More likely, the doping decreases the spin correlation length ξ along a chain, and therefore inhibits both the weak interplane coupling (possibly at very low x) and the collective interchain coupling (at moderate x). The $x = 1$ data may thus be indicative of 1D Heisenberg chain behavior; this possibility is illustrated in the lattice-subtracted specific heat of Fig. 2(b), with the theoretical curve [19] for an infinite 1D Heisenberg chain with a single fitting parameter $J \approx 27$ K shown by the dotted line. It may also be that intrachain (J) and interchain (J') couplings are both important, but that the nonmagnetic Zhang-Rice singlets [20] are arranged as suggested in Fig. 3(a1), where for $x = 1$, four-spin segments couple to form long chains that produce the observed 1D behavior. In either scenario, the magnitude and broadness of the $x = 1$ heat capacity can be accounted for by considering a transition to 1D behavior as holes are introduced into the chains.

Even more interesting is the behavior as the doping level increases to the maximally doped value of 0.4 holes/Cu ($x = 2$), where a broad specific heat peak at $T \approx 25$ K is accompanied by another maximum at $T \approx 11$ K. This temperature coincides with the shoulder in the susceptibility discussed previously. In $Ca_4Cu_5O_{10}$, $\frac{2}{5}$ of the CuO_2 squares have become nonmagnetic, again most likely due to the formation of Zhang-Rice singlets. The low-temperature peak in the specific heat and the shoulder in the magnetic susceptibility indicate that the behavior of

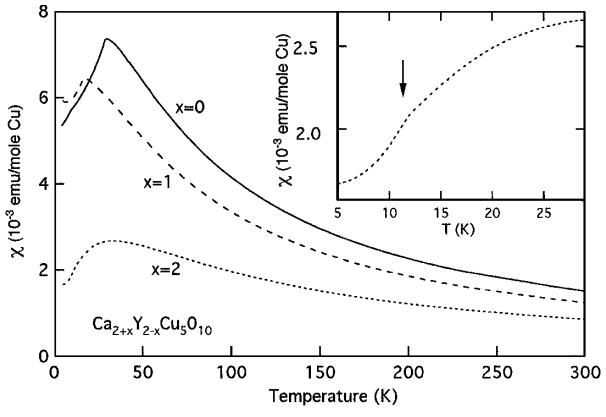

FIG. 1. Magnetic susceptibility vs temperature for $Ca_{2+x}Y_{2-x}Cu_5O_{10}$ for $x = 0$ (solid line), $x = 1$ (long-dashed line), and $x = 2$ (short-dashed line). Inset: Shoulder at $T \approx 11$ K for $Ca_4Cu_5O_{10}$.

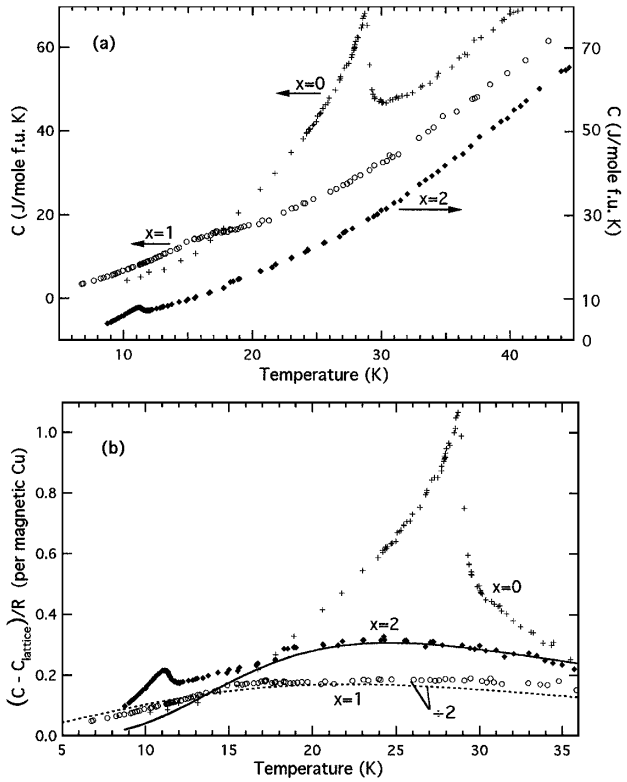

FIG. 2. (a) Specific heat per mole formula unit vs temperature for $Ca_{2+x}Y_{2-x}Cu_5O_{10}$ for $x = 0$, 1, and 2. (b) Lattice-subtracted specific heat (in units of $R = N_A k_B$) per magnetic copper (experimental points), specific heat of infinite 1D Heisenberg chain (dashed line), and dimer specific heat (solid line).

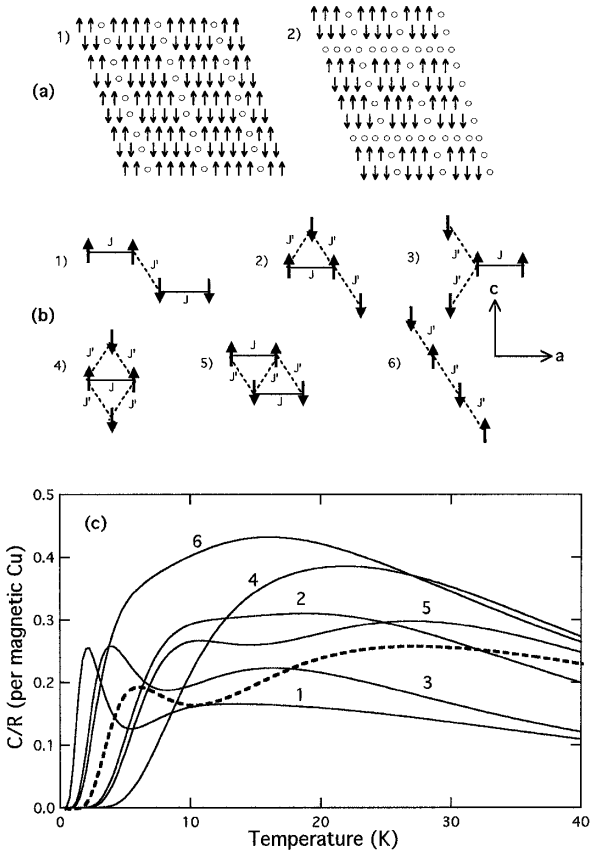

FIG. 3. (a) Possible configurations for doping levels $x = 1$ (1D chains) and $x = 2$ (12-spin clusters). (b) Six 4-spin cluster configurations with only nearest neighbor interactions which have vanishing low-temperature susceptibility for $J < 0$ and $J' > 0$. (c) Specific heat calculated by exact diagonalization vs temperature showing the double-peak behavior for the six 4-spin cluster configurations of (b); these examples use the values $J = -30$ K for the intrachain coupling and $J' = 20$ K for the interchain coupling. Also shown is a 3:1 superposition of cluster configurations 3 and 4 (thick line).

the three remaining magnetically active Cu per formula unit cannot be described by a simple dilution of spins resulting in isolated dimers. This is illustrated by the solid line in Fig. 2(b), which shows the lattice-subtracted specific heat of $Ca_4Cu_5O_{10}$ along with the specific heat expected for an ensemble of isolated spin-$\frac{1}{2}$ dimers [21]:

$$C = \frac{6N(J/T)^2 \exp(-2J/T)}{[1 + 3\exp(-2J/T)]^2}, \qquad (1)$$

where $N = \frac{3}{5}$ is fixed by the doping level, and a single fitting parameter, $J = 34$ K, has been used. It is clear that the dimer fit cannot account for the peak at $T = 11$ K. Next nearest neighbor interactions within a chain (e.g., two dimers coupled across a Zhang-Rice singlet) produce observable effects in $Sr_{14}Cu_{24}O_{41}$, but are reduced in strength by $J_{nnn}/J \approx 0.07$ [22], and so may only be observable in the present system below $T \approx 0.07J/k_B \approx 2$ K. Much stronger in $Ca_{2+x}Y_{2-x}Cu_5O_{10}$ is the interchain coupling, J'.

We thus consider the possibility that the behavior may be described by an ensemble of finite spin clusters with $N > 2$. Only even-number clusters need to be considered because of the vanishing behavior of the low-temperature magnetic susceptibility. In order to fix both the number of spins and the number of lattice sites, large clusters with $N \approx 12$, like those depicted in configuration 2 of Fig. 3(a), would have to form for $x = 2$. However, for simplicity, we consider only clusters with $N = 4$. Because of errors in a vector model of spin clusters in the literature [23], the specific heat of four-spin cluster configurations for staggered chains was calculated by exact diagonalization of the Heisenberg Hamiltonian:

$$H = 2\sum_{i=1}^{3}\sum_{j=i+1}^{4} J_{ij}\mathbf{S}_i \cdot \mathbf{S}_j, \qquad (2)$$

where $J_{ij} = J$ for neighboring spins in the same chain, $J_{ij} = J'$ for neighboring spins in adjacent chains, and $J_{ij} = 0$ otherwise. It is believed [16,17] that the intrachain coupling is ferromagnetic ($J < 0$) while the interchain coupling is antiferromagnetic ($J' > 0$). Therefore, only clusters which have a vanishing low-temperature susceptibility when $J < 0$ and $J' > 0$ are discussed here. Of the nine unique configurations, Fig. 3(b) shows the six which fit this criteria. Figure 3(c) shows the results of the exact specific heat calculations of these various four-spin cluster configurations, where we have chosen $J = -30$ K and $J' = 20$ K for illustrative purposes. For some clusters, the exact diagonalization calculation results in a low-lying pair of energy levels, producing the lower-temperature specific heat peak. It is evident that, although the location and relative heights of the double peaks do not account exactly for the observed behavior, the specific heat resulting from the four-spin cluster configurations has a temperature dependence and magnitude similar to the measured data. Configuration 5 alone, the simple parallelogram cluster, provides a good approximation to the data. The observed double-peak behavior can also be closely approximated by a superposition of configurations 3 and 4, with $J = -45$ K and $J' = 30$ K, as indicated in Fig. 3(c). The remaining deviations may be due to anisotropy terms in the Hamiltonian, or may reflect the need to invoke larger clusters like the 12-spin cluster of Fig. 3(a2) mentioned above. Thus we propose that as the doping level increases from $x = 1$ to $x = 2$ there is a transition from one-dimensional to zero-dimensional behavior, that is, to microscopic segregation into finite spin clusters, with Zhang-Rice singlets forming the boundaries, or "stripes," around these clusters [24].

In order to better understand the magnetic properties of $Ca_{2+x}Y_{2-x}Cu_5O_{10}$, the anisotropy of the system was investigated. X-ray diffraction and susceptibility results on grain-aligned samples in epoxy (Fig. 4) indicate that the crystallographic b axis, perpendicular to the planes containing the chains, is the easy axis, confirming a previous result for $x = 0$ [25]. New results were obtained in

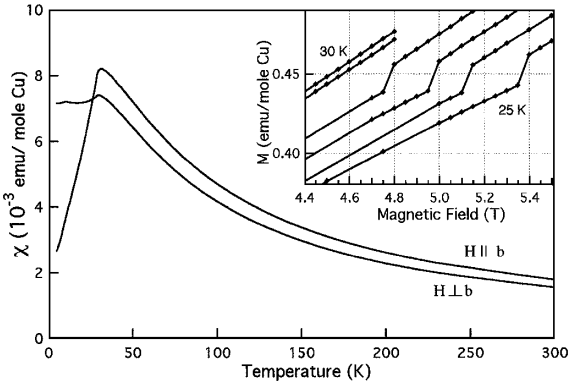

FIG. 4. Magnetic susceptibility vs temperature for grain-aligned $Ca_2Y_2Cu_5O_{10}$ showing easy axis of magnetization parallel to the crystallographic b axis. Inset: Spin-flop transition observed below 29 K; data are for 1 K increments from 25 to 30 K.

the present study for the other doping levels that indicate that the easy axis does not change as holes are introduced into the chains; however, the susceptibility data from grain-aligned samples of the very reactive, doped concentrations are dominated by Curie tails from ions dissolved in epoxy and are not shown here. The inset of Fig. 4 shows isothermal magnetization data as a function of field at various temperatures. Because of our maximum field (5.5 T), no field-dependent anisotropy features were observed for temperatures below 25 K. However, measurements made for 25 K $\leq T < T_N$ show spin-flop transitions, with H_{SF} decreasing as temperature increases. The data of the Fig. 4 inset suggest the presence of a bicritical line between Ising and XY anisotropy, which may be useful for tuning the effective anisotropy to zero [26]. A linear extrapolation of the data provides the value $H_{\mathrm{SF}}(0) = 10.3 \pm 0.6$ T; in a mean-field model, the relation $H_{\mathrm{SF}}(0) = (2H_E H_A - H_A^2)^{1/2}$, along with an estimate of the exchange field, $H_E = 2ZJS/g\mu_B \approx 90$ T (for $J = 30$ K), provides a measure of the anisotropy field, $H_A \approx 0.59$ T. Notice that H_{SF} does not approach zero as T approaches T_N, indicating strong magnetic correlations above T_N.

In summary, we have investigated the magnetic behavior of the spin-chain compound $Ca_{2+x}Y_{2-x}Cu_5O_{10}$ over a wide range of hole doping. We support earlier findings of long-range antiferromagnetism in the undoped compound, with $T_N = 29$ K. Using quantitative analysis of specific heat measurements, we examined the nature of the magnetic behavior for the hole-doped compounds. We find a possible transition to 1D Heisenberg chain behavior for the $x = 1$ compound. Furthermore, we find that the experimental results for the maximally hole-doped $Ca_4Cu_5O_{10}$ can be understood in a framework of microscopic segregation into isolated finite spin clusters, indicating a second doping-induced dimensionality transition between $x = 1$ and $x = 2$. Also, the magnetic anisotropy was determined and a spin-flop transition observed. Materials efforts are now underway to further extend the hole concentration using alkali doping, which was previously found to be successful in planar La_2CuO_4 [27].

This work was supported by the U.S. National Science Foundation under Grant No. DMR-9705414 and the Robert A. Welch Foundation under Grant No. F-1191.

[1] K. M. Kojima *et al.,* Phys. Rev. Lett. **78**, 1787 (1997).
[2] N. Motoyama, H. Eisaki, and S. Uchida, Phys. Rev. Lett. **76**, 3212 (1996).
[3] M. Hase, I. Terasaki, and K. Uchinokura, Phys. Rev. Lett. **70**, 3651 (1993).
[4] P. E. Anderson, J. Z. Liu, and R. N. Shelton, Phys. Rev. B **57**, 11 492 (1998).
[5] P. E. Anderson, J. Z. Liu, and R. N. Shelton, Phys. Rev. B **56**, 11 014 (1997).
[6] M. Matsuda and K. Katsumata, Phys. Rev. B **53**, 12 201 (1996).
[7] S. A. Carter *et al.,* Phys. Rev. Lett. **77**, 1378 (1996).
[8] T. Imai *et al.,* Phys. Rev. Lett. **81**, 220 (1998).
[9] A. Shengelaya *et al.,* Phys. Rev. Lett. **80**, 3626 (1998).
[10] G. I. Meijer *et al.,* Phys. Rev. B **58**, 14 452 (1998).
[11] J. Dolinsek *et al.,* Phys. Rev. B **57**, 7798 (1998).
[12] G. I. Meijer *et al.,* Europhys. Lett. **42**, 339 (1998).
[13] A. Hayashi, B. Batlogg, and R. J. Cava, Phys. Rev. B **58**, 2678 (1998).
[14] P. K. Davies, Solid State Chem. **95**, 365 (1991).
[15] K. K. Singh, D. E. Morris, and A. P. B. Sinha, Physica (Amsterdam) **231C**, 377 (1994).
[16] H. F. Fong *et al.,* Phys. Rev. B **59**, 6873 (1999).
[17] M. Matsuda, K. Ohoyama, and M. Ohashi, J. Phys. Soc. Jpn. **68**, 269 (1998).
[18] R. Bachmann *et al.,* Rev. Sci. Instrum. **43**, 205 (1972).
[19] R. L. Carlin, *Magnetochemistry* (Springer-Verlag, Berlin, 1986), Chap. 7.
[20] F. C. Zhang and T. M. Rice, Phys. Rev. B **37**, 3759 (1988).
[21] M. Matsuda *et al.,* Phys. Rev. B **59**, 1060 (1999).
[22] R. L. Carlin, *Magnetochemistry* (Ref. [19]), Chap. 5.
[23] S. J. Gruber, C. M. Harris, and E. Sinn, J. Chem. Phys. **49**, 2183 (1968).
[24] J. Tranquada *et al.,* Nature (London) **375**, 561 (1995).
[25] H. Yamaguchi, K. Oka, and T. Ita, Physica (Amsterdam) **320C**, 167 (1999).
[26] R. L. Leheny, R. J. Christianson, and R. J. Birgeneau, Phys. Rev. Lett. **82**, 418 (1999).
[27] J. T. Markert *et al.,* Solid State Commun. **66**, 387 (1988).